Supplementary Information for:

High Expression of Integrin αvβ3 Enables Uptake of Targeted Fluorescent Probes into Ovarian Cancer Cells and Tumors

Scott K. Shaw, Cynthia L. Schreiber, Felicia M. Roland, Paul M. Battles, Seamus P. Brennan, Simon J. Padanilam, Bradley D. Smith*

Department of Chemistry and Biochemistry, 236 Nieuwland Science Hall, University of Notre Dame, Notre Dame, IN 46556, USA

**Email: smith.115@nd.edu*

Section 1: Synthesis and Characterization

Synthesis of cRGD

The linear peptide was prepared by standard solid phase methods. The peptide cyclization was performed by slowly adding a solution of the linear peptide acetate salt in 12 mL of DCM to a solution of 50% 1-propanephosphonic acid cyclic anhydride (T3P) in EtOAc (3.2 mL), triethyl amine (TEA, 3.7 mL), and DMAP (12 mg) in 500mL of DCM. After stirring overnight, the starting material could not be detected by RP-HPLC. The reaction mixture was concentrated and purified by flash chromatography (methanol:ethyl acetate, 1:10) to afford 161 mg of the protected cyclic peptide as a light yellow solid. The protecting groups were removed with a mixture of water and trifluoroacetic acid (TFA) (1:19). After removal of the solvent, the residue was triturated with diethyl ether followed by filtration to yield cRGD as the TFA salt (MW=831.72, 121 mg, 92.0%) as a light yellow powder. **^{1}H-NMR** (600 MHz; D_2O): δ 7.36 (t, *J* = 7.4 Hz, 2H), 7.30 (t, *J* = 7.4 Hz, 1H), 7.25 (d, *J* = 7.2 Hz, 2H), 4.76 (dd, *J* = 7.6, 6.8 Hz, 1H), 4.61 (dd, *J* = 10.0, 6.2 Hz, 1H), 4.34 (dd, *J* = 8.8, 6.0 Hz, 1H), 4.17 (d, *J* = 15.0 Hz, 1H), 3.88 (dd, *J* = 10.6, 4.4 Hz, 1H), 3.49 (d, *J* = 15.0 Hz, 1H), 3.17 (quintet, *J* = 7.1 Hz, 3H), 3.06 (dd, *J* = 13.2, 6.1 Hz, 1H), 2.97-2.85 (m, 4H), 2.73 (dd, *J* = 16.8, 6.5 Hz, 1H), 1.84 (t, *J* = 3.2 Hz, 1H), 1.65 (td, *J* = 9.4, 5.2 Hz, 2H), 1.50 (tdd, *J* = 14.7, 8.3, 6.6 Hz, 5H), 1.26 (t, *J* = 7.3 Hz, 1H), 1.16 (t, *J* = 7.1 Hz, 1H), 0.96 (dd, *J* = 15.4, 6.5 Hz, 2H). **LCMS (ESI-TOF):** calculated for $C_{27}H_{42}N_9O_7$ $[M+H]^+$ 604.3202, found 604.3226.

Synthesis of Squaraine Probes

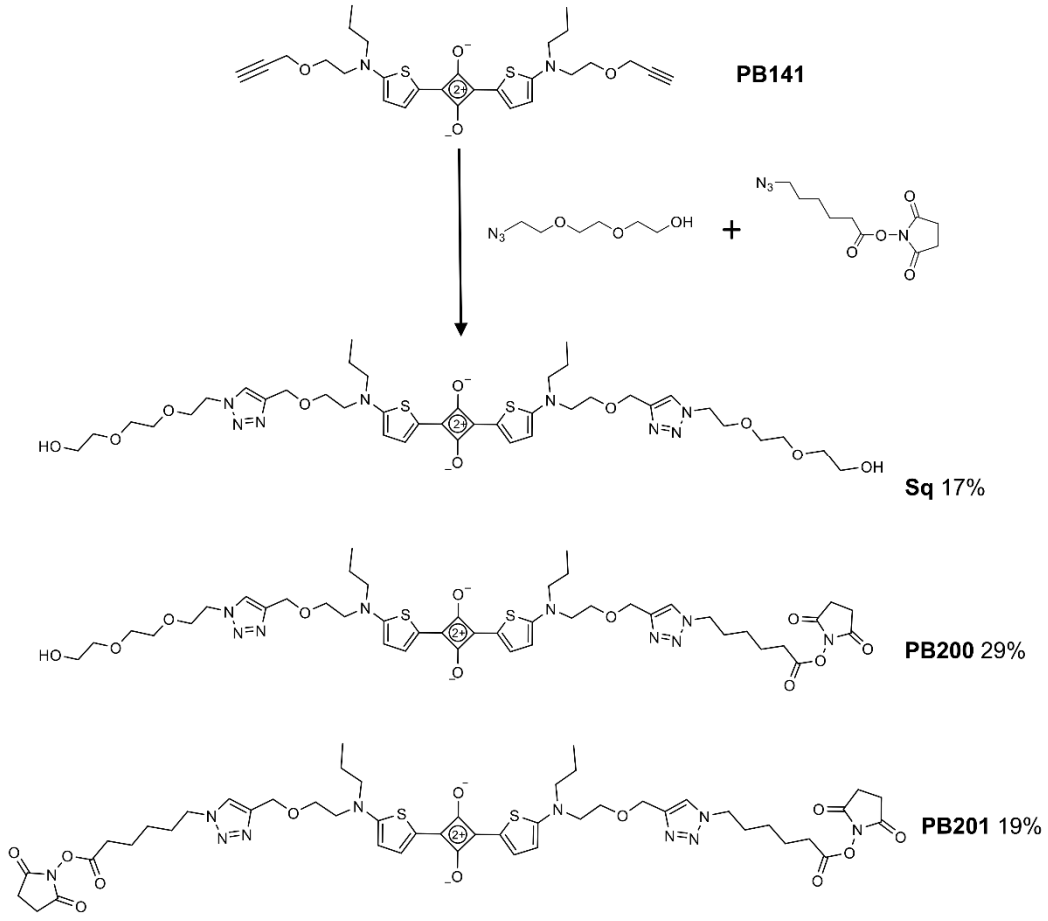

Scheme S1

PB141 (50mg, 0.1mmol), triethylene glycol azide (16.7mg, 0.1mmol), 6-azidohexanoic acid succinimido ester (24.2mg, 0.1mmol), Cu(I)TBTA-Br (16mg, 25 mol%) and DIPEA (50µL, 0.3mmol) were dissolved in $CHCl_3$ (5mL) and stirred at room temperature for 16 hours. The solvent was removed *in vacuo* and the resulting residue purified by gradient silica gel column chromatography using 10% MeOH/DCM to elute the products as a bright blue solid.

Sq. (14mg, 17%). **^{1}H-NMR** (500 MHz; $CDCl_3$): δ 7.92 (dd, *J* = 4.6, 3.7 Hz, 1H), 7.71 (s, 1H), 6.25 (d, *J* = 4.6 Hz, 1H), 4.63 (s, 1H), 4.51 (t, *J* = 5.0 Hz, 1H), 4.15 (d, *J* = 2.4 Hz, 1H), 3.83 (t, *J* = 5.0 Hz, 1H), 3.78 (q, *J* = 5.1 Hz, 2H), 3.72-3.71 (m, 1H), 3.66 (dt, *J* = 14.8, 5.4 Hz, 2H), 3.59-3.54 (m, 3H), 3.49-3.46 (m, 1H), 3.42 (t, *J* = 7.7 Hz, 1H), 2.44 (t, *J* = 2.3 Hz,), 1.76-1.68 (m, 2H), 1.39 (t, *J* = 7.3 Hz, 1H), 0.97-0.91 (m, 3H). **HRMS (ESI-TOF):** calculated for $C_{40}H_{59}N_8O_{10}S_2$ $[M+H]^+$ 875.3790, found 875.3807. (**ABS_λ**=663, **Fl_λ**(676)**Φ** =0.02, **log(ε)**= 5.35)

PB200. (26.1mg, 29%) **^{1}H-NMR** ^{1}H-NMR (500 MHz; $CDCl_3$): δ 7.91 (t, *J* = 5.0 Hz, 2H), 7.72 (s, 1H), 7.51 (s, 1H), 6.25 (dd, *J* = 7.7, 4.8 Hz, 2H), 4.63 (s, 4H), 4.52 (t, *J* = 4.9 Hz, 2H), 4.33 (t, *J* = 7.2 Hz, 2H), 3.83 (t, *J* = 5.0 Hz, 2H), 3.78 (t, *J* = 5.2 Hz, 4H), 3.72 (t, *J* = 4.5 Hz, 2H), 3.66 (q, *J* = 5.9 Hz, 4H), 3.58-3.54 (m, 6H), 3.43 (t, *J* = 7.4 Hz, 4H), 2.83 (s, 4H), 2.57 (t, *J* = 7.2 Hz, 2H), 1.91 (t, *J* = 7.6 Hz, 2H), 1.73 (dq, *J* = 21.6, 7.4 Hz, 6H), 1.42 (s, 2H), 0.93 (t, *J* = 7.3 Hz, 6H). **HRMS (ESI-TOF):** calculated for $C_{44}H_{59}N_9NaO_{11}S_2$ $[M+Na]^+$ 976.3667, found 976.3642.

PB201. (15.5mg, 19%).**^{1}H-NMR** (600 MHz; $CDCl_3$): δ 7.92 (d, *J* = 4.7 Hz, 2H), 7.50 (s, 2H), 6.25 (d, *J* = 4.7 Hz, 2H), 5.29-5.29 (m, 3H), 4.63 (d, *J* = 2.7 Hz, 4H), 4.33 (t, *J* = 7.2 Hz, 4H), 3.78 (t, *J* = 5.4 Hz, 4H), 3.66 (t, *J* = 5.3 Hz, 4H), 3.45 (dt, *J* = 14.1, 7.2 Hz, 5H), 2.83 (s, 8H), 2.57 (t, *J* = 7.2 Hz, 4H), 1.91 (t, *J* = 7.5 Hz, 4H), 1.73 (dq, *J* = 23.8, 7.8 Hz, 10H), 1.44-1.41 (m, 6H), 0.94 (t, *J* = 7.4 Hz, 6H). **HRMS (ESI-TOF):** calculated for $C_{48}H_{60}N_{10}NaO_{12}S_2$ $[M+Na]^+$ 1055.3725, found 1055.3723.

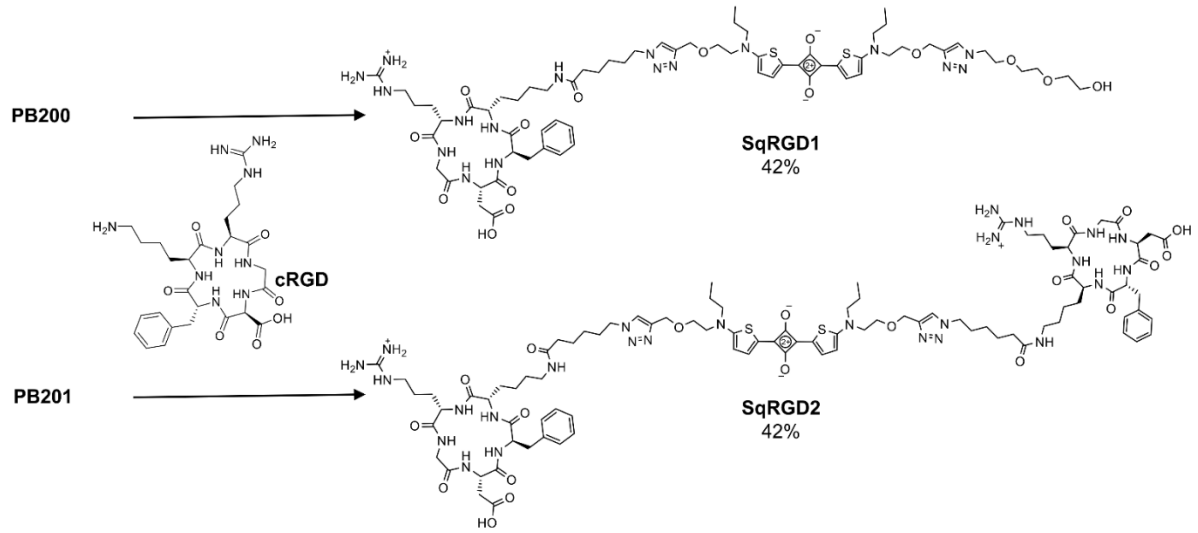

Scheme S2

SqRGD1. PB200 (25mg, 0.2mmol), cRGD (36mg, 0.2mmol), DIPEA (72µL, 0.4mmol) were dissolved in DMF (10mL) and stirred at room temperature for 24 hours. The solvent was removed *in vacuo* and the resulting residue purified by reverse phase column chromatography using 30% MeCN/Water 0.1%TFA to elute the product as a bright blue solid (12mg, 42%).**^{1}H-NMR** (600 MHz; D_2O): δ 8.65-8.64 (m, 1H), 8.61-8.58 (m, 2H), 8.56-8.54 (m, 1H), 8.48-8.46 (m, 1H), 8.40-8.38 (m, 1H), 8.16-8.14 (m, 1H), 8.08-8.06 (m, 1H), 7.99-7.96 (m, 2H), 7.92-7.89 (m, 3H), 5.40-5.38 (m, 1H), 5.32-5.27 (m, 5H), 5.22-5.19 (m, 2H), 5.01-4.97 (m, 2H), 4.94-4.91 (m, 1H), 4.89-4.85 (m, 1H), 4.61-4.56 (m, 2H), 4.56-4.50 (m, 3H), 4.30-4.26 (m, 2H), 4.26-4.19 (m, 5H), 4.17-4.14 (m, 2H), 4.12-4.09 (m, 1H), 3.87-3.77 (m, 2H), 3.73-3.67 (m, 2H), 3.66-3.63 (m, 3H), 3.53-3.49 (m, 1H), 3.31-3.28 (m, 1H), 2.81-2.76 (m, 2H), 2.56-2.44 (m, 4H), 2.44-2.25

(m, 6H), 2.25-2.11 (m, 6H), 2.03-1.98 (m, 2H), 1.90-1.85 (m, 2H), 1.75-1.51 (m, 7H). **HRMS (ESI-TOF):** calculated for $C_{67}H_{96}N_{17}O_{15}S_2$ $[M+H]^+$ 1442.6707, found 1442.6723. (**ABS$_\lambda$**=665, **FI$_\lambda$**(678)**Φ**=0.03, **log(ε)**= 5.25)

SqRGD2. PB201 (10mg, 0.01mmol), cRGD (17.7mg, 0.02mmol), DIPEA (10µL, 0.06mmol) were dissolved in DMF (10mL) and stirred at room temperature for 24 hours. The solvent was removed *in vacuo* and the resulting residue purified by reverse phase column chromatography using 30% MeCN/Water 0.1%TFA to elute the product as a bright blue solid (9mg, 42%).**^{1}H-NMR** (600 MHz; CD_3CN): δ 8.20 (dd, *J* = 2.7, 1.6 Hz, 1H), 8.16 (s, 1H), 7.67 (td, *J* = 6.7, 1.5 Hz, 2H), 7.61-7.57 (m, 3H), 5.10 (dd, *J* = 8.0, 6.2 Hz, 1H), 4.99-4.97 (m, 3H), 4.68 (td, *J* = 6.8, 3.3 Hz, 3H), 4.64 (dd, *J* = 9.3, 5.4 Hz, 1H), 4.57 (d, *J* = 15.2 Hz, 2H), 4.27 (dd, *J* = 10.3, 4.5 Hz, 1H), 4.19-4.17 (m, 4H), 3.82 (d, *J* = 15.2 Hz, 2H), 3.55-3.50 (m, 3H), 3.41-3.31 (m, 5H), 3.23 (dd, *J* = 16.8, 8.0 Hz, 1H), 3.02 (dd, *J* = 16.8, 6.2 Hz, 1H), 2.48 (t, *J* = 7.5 Hz, 2H), 2.17 (t, *J* = 7.4 Hz, 4H), 2.08-2.06 (m, 2H), 2.01-1.97 (m, 3H), 1.92-1.84 (m, 6H), 1.71-1.67 (m, 3H), 1.57-1.55 (m, 2H), 1.38-1.35 (m, 2H), 1.31-1.28 (m, 3H).
HRMS (ESI-TOF): calculated for $C_{94}H_{133}N_{26}O_{20}S_2$ $[M+H]^+$ 2009.9625, found 2009.9601.
(**ABS$_\lambda$**=667, **FI$_\lambda$**(679) =0.05, **log(ε)**= 4.90)

Probe	ABS (nm)	FI (nm)	FI QY	log[ε]	Brightness
Sq	663	676	0.02	5.35	5×10^3
SqRGD1	665	678	0.03	5.25	5×10^3
SqRGD2	667	679	0.05	4.90	4×10^3

Table S1: Spectral properties of squaraine probes. Spectral data for absorption and emission maxima bands were taken in 25 mM MOPS buffer, pH 7.2 at 3.0 µM. Brightness is defined as the product of quantum yield (QY) and the molar absorptivity.

The squaraine dyes exist as two conformational isomers, based on the relative orientation of the thiophene units (*cis* or *trans*) and this leads to complicated NMR patterns. Furthermore, in some samples (e.g., SqRGD1) the rate of squaraine isomerism is similar to the NMR timescale and due to exchange broadening the thiophene signals at ~6.5 ppm are too broad to be observed.

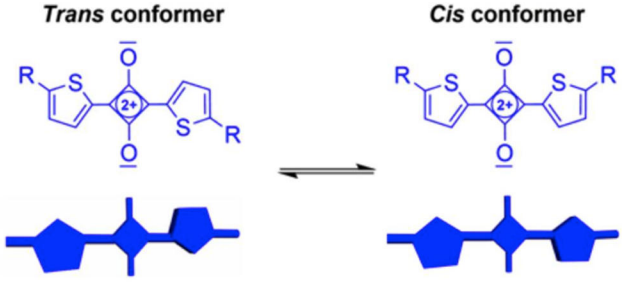

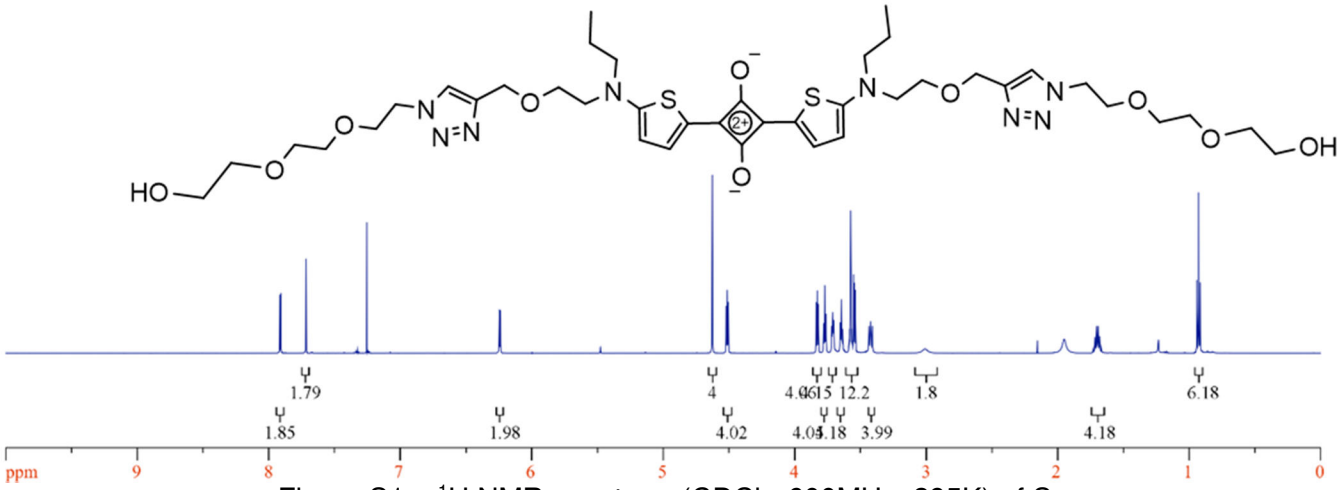

Figure S1a: ^{1}H NMR spectrum ($CDCl_3$, 600MHz, 295K) of Sq

Mass Spectrometry & Proteomics Facility

Mass Spectrum SmartFormula Report

Analysis Info

Analysis Name	D:\Data\0928\43792-PB151.d	Acquisition Date	9/28/2015 3:11:09 PM
Method	Tune_high_pos.m	Operator	nsevova
Sample Name	PB151	Instrument / Ser#	micrOTOF 213750.10 314
Comment			

Acquisition Parameter

Source Type	ESI	Ion Polarity	Positive	Set Nebulizer	0.3 Bar
Focus	Not active	Set Capillary	4500 V	Set Dry Heater	180 °C
Scan Begin	50 m/z	Set End Plate Offset	-500 V	Set Dry Gas	4.0 l/min
Scan End	3000 m/z	n/a	n/a	Set Divert Valve	Source

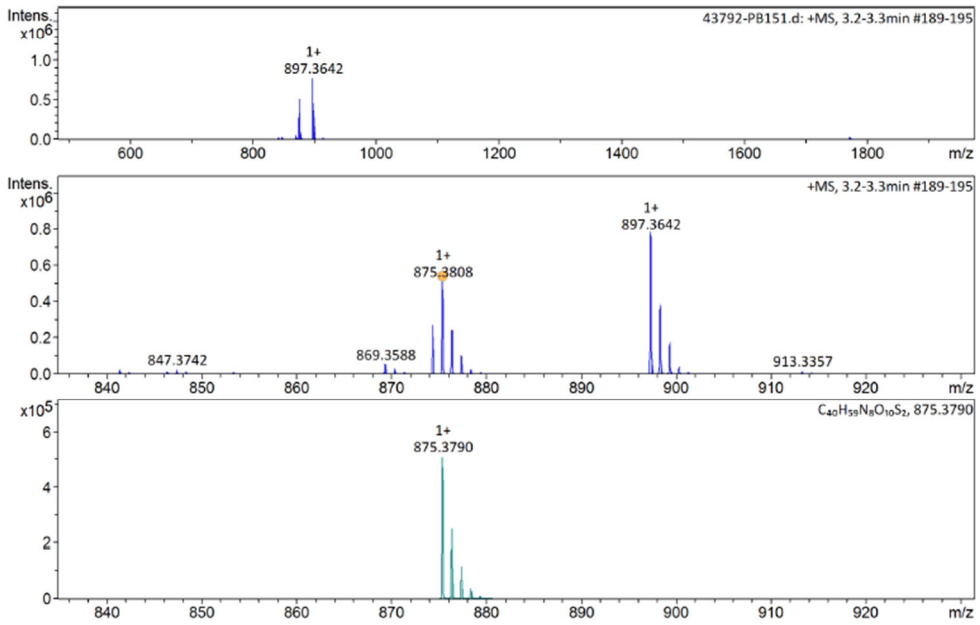

Meas. m/z	#	Ion Formula	m/z	err [ppm]	Mean err [ppm]	rdb	N-Rule	e⁻ Conf	mSigma	Std I	Std Mean m/z	Std I VarNorm	Std m/z Diff	Std Comb Dev
875.380755	1	C40H59N8O10S2	875.379009	-2.0	-2.1	15.5	ok	even	19.5	31.7	n.a.	n.a.	n.a.	n.a.

Figure S1b: HRMS (ESI-TOF) of Sq

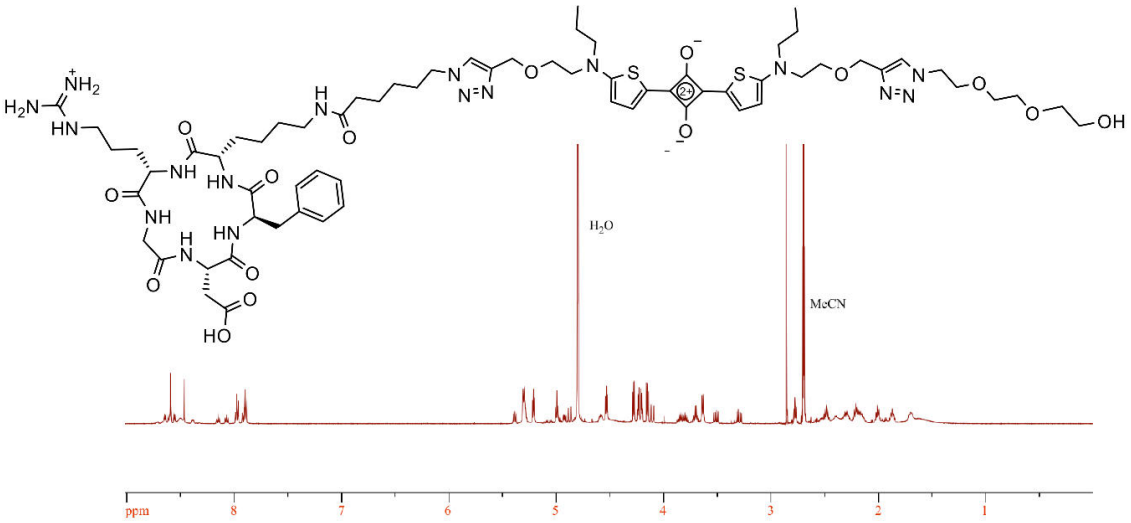

Figure S2a: ^{1}H NMR spectrum (D_2O, 600MHz, 295K) of SqRGD1.

Mass Spectrometry & Proteomics Facility

Mass Spectrum SmartFormula Report

Analysis Info

Analysis Name	D:\Data\1125\46744-PB209.d	Acquisition Date	11/25/2015 1:58:33 PM
Method	Tune_high_pos.m	Operator	nsevova
Sample Name	PB209	Instrument / Ser#	micrOTOF 213750.10 314
Comment			

Acquisition Parameter

Source Type	ESI	Ion Polarity	Positive	Set Nebulizer	0.3 Bar
Focus	Not active	Set Capillary	4500 V	Set Dry Heater	180 °C
Scan Begin	50 m/z	Set End Plate Offset	-500 V	Set Dry Gas	4.0 l/min
Scan End	3000 m/z	n/a	n/a	Set Divert Valve	Source

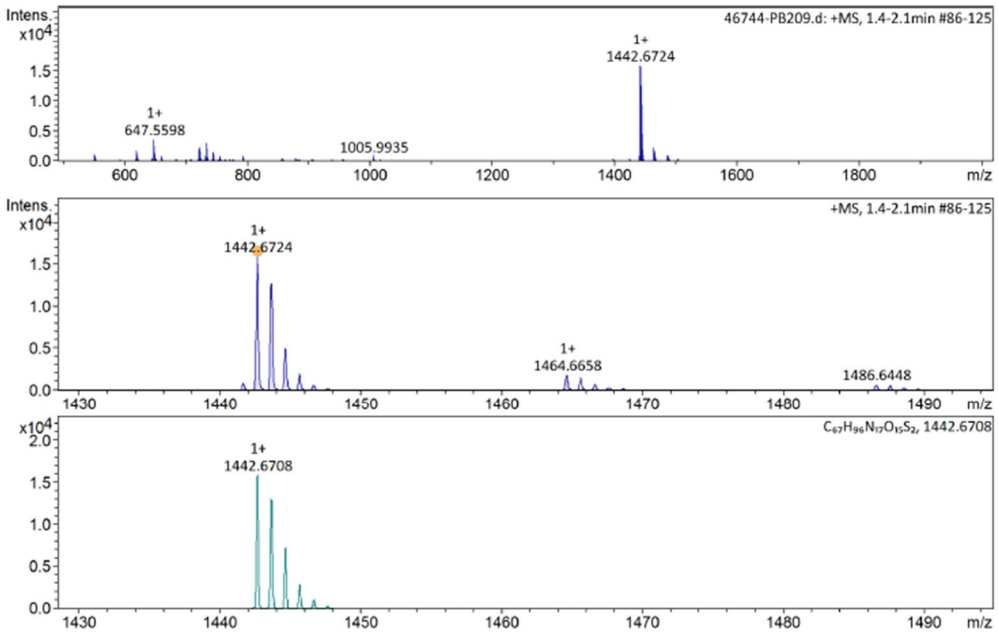

Meas. m/z	#	Ion Formula	m/z	err [ppm]	Mean err [ppm]	rdb	N-Rule	e⁻ Conf	mSigma	Std I a	Std Mean m/z	Std I VarNorm	Std m/z Diff	Std Comb Dev
1442.672385	1	C67H96N17O15S2	1442.670774	-1.1	555.0	28.5	ok	even	98.4	125.3	n.a.	n.a.	n.a.	n.a.

Figure S2b: HRMS (ESI-TOF) of SqRGD1

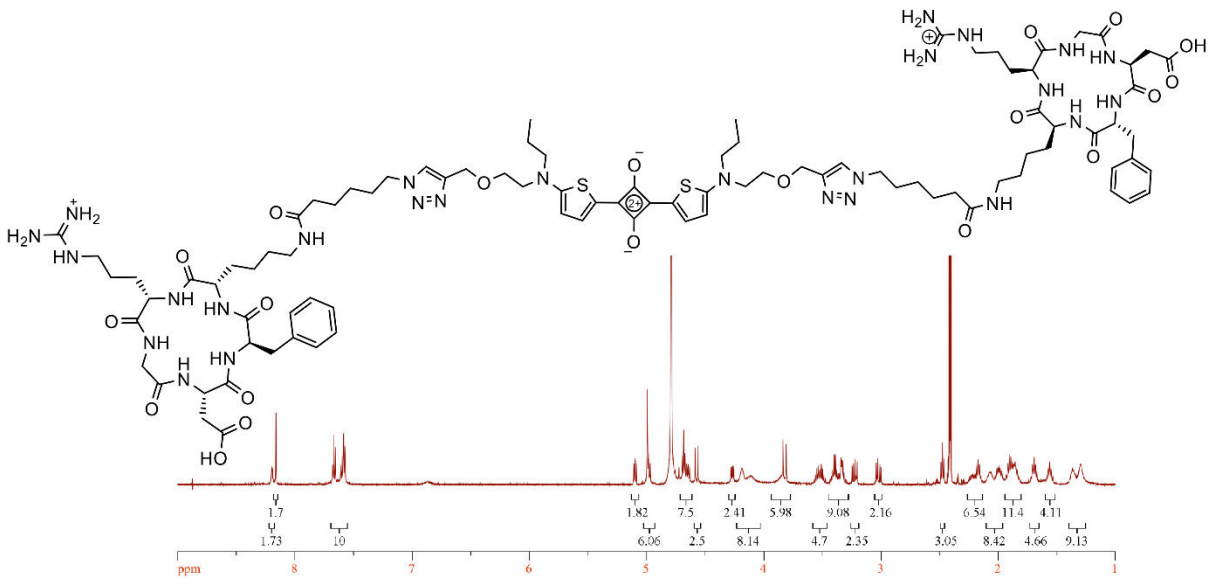

Figure S3a: ^{1}H NMR spectrum (CD_3CN, 600MHz, 295K) of SqRGD2

Mass Spectrometry & Proteomics Facility

Mass Spectrum SmartFormula Report

Analysis Info

Analysis Name	D:\Data\1125\46744-PB208.d	Acquisition Date	11/25/2015 1:51:00 PM
Method	Tune_high_pos.m	Operator	nsevova
Sample Name	PB208	Instrument / Ser#	micrOTOF 213750.10314
Comment			

Acquisition Parameter

Source Type	ESI	Ion Polarity	Positive	Set Nebulizer	0.3 Bar
Focus	Not active	Set Capillary	4500 V	Set Dry Heater	180 °C
Scan Begin	50 m/z	Set End Plate Offset	-500 V	Set Dry Gas	4.0 l/min
Scan End	3000 m/z	n/a	n/a	Set Divert Valve	Source

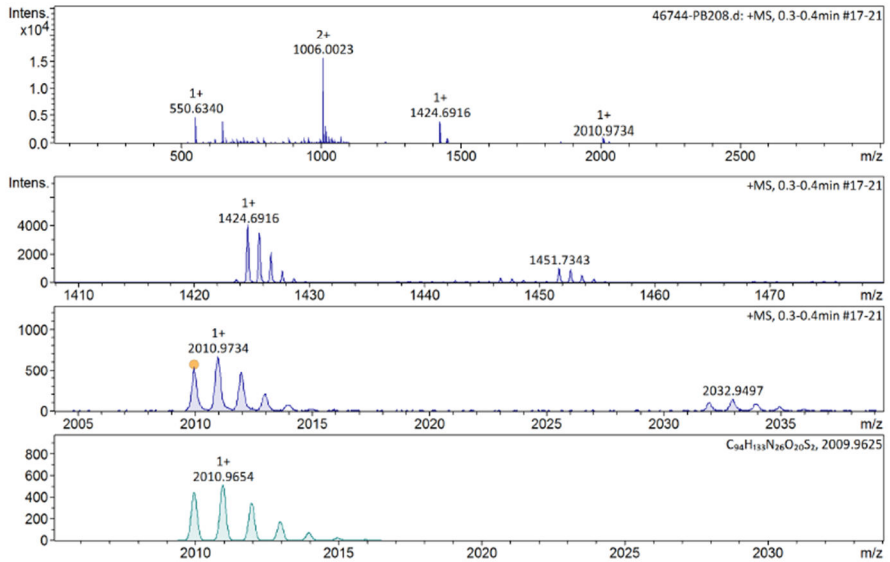

Meas. m/z	#	Ion Formula	m/z	err [ppm]	Mean err [ppm]	rdb	N-Rule	e⁻ Conf	mSigma	Std I	Std Mean m/z	Std I Var Norm	Std m/z Diff	Std Comb Dev
2009.960113	1	C94H133N26O20S2	2009.962539	1.2	1140.9	41.5	ok	even	n.a.	827.7	n.a.	n.a.	n.a.	n.a.

Figure S3b: HRMS (ESI-TOF) of SqRGD2

Section 2: Integrin Receptor Quantification

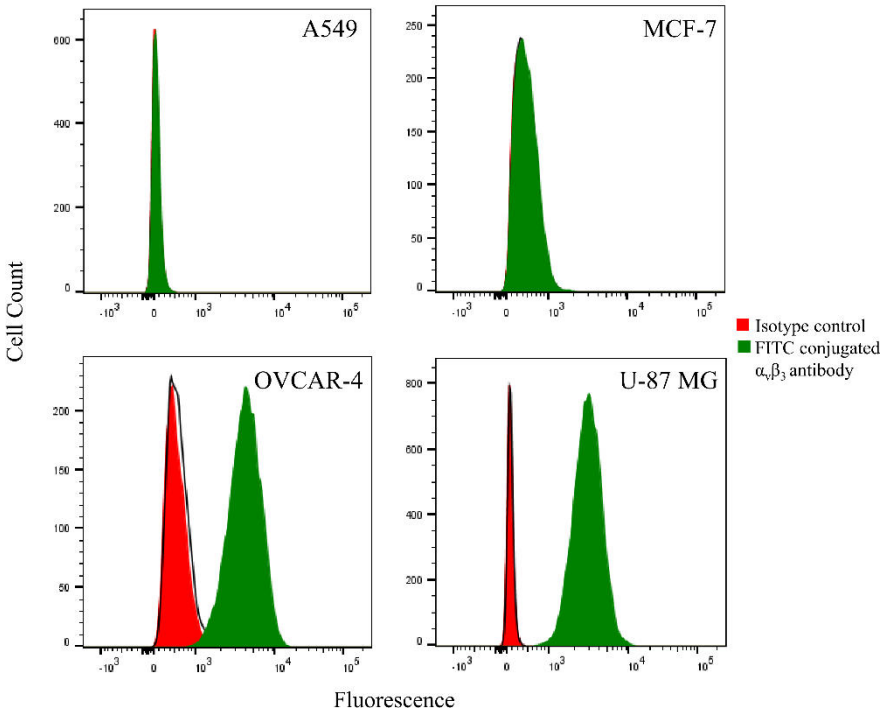

Figure S4: Flow cytometry assessment of αvβ3 expression by staining with fluorescent FITC conjugated αvβ3 antibody: (top) αvβ3 negative A549 and MCF-7 cells, (bottom) αvβ3 positive OVCAR-4 and U-87 MG cells.

Cell Surface Area Measurements

Measurements of surface area are uncommon in the literature, and when done typically rely on simply geometric estimation based of average cell diameter as measured by flow cytometry backscattering. For example, A549 cells measured in this manner were estimated to have a surface area of 710 um^2 (S1). However these estimates are limited in that they can only be done on detached, rounded cells suspended in solution. Also they do not account for the highly irregular geometry seen in attached cells, including indentations, projections and ruffles, which greatly inflate the surface area (S2). Computer aided 3-D image cytometry of cells is emerging as a more realistic method for measurement of cell geometrical characteristics such as volume and surface area. The technique involves the digital reconstruction of high-resolution image stacks obtained by confocal laser scanning microscopy (CLSM) from serial sections of a cell (S3). For this technique, care should be taken to avoid artificial inflation of surface area due to inclusions of extracellular artifacts in the 3-D model or distortion of images by noise (4). The membrane stain DiI helped avoid artifacts, as the dye sequestered cleanly into the cell membrane leaving a clear delineation between the cell and its surroundings. Surface area inflation due to noise was minimized by smoothing with 3-D Gaussian filtration, and only a <3% difference in the surface area of a cell reconstructed from a smoothed vs a not-smoothed image stack was observed. Another limitation is the underestimation of surface area when cells are clustered and their membranes apposed. For this study, only single cells or small (less than 3) cell clusters were analyzed. For the clusters, it was estimated (by manual segmentation of the image stacks at the approximate cell boundaries) the hidden surface area accounts for <2% of the reported surface area. We have not found previous measurements of cell surface area by this technique for the specific cell lines used in this study, but our surface area measurements are commensurate to the value of 2600 μM^2 reported by this technique for HEK293, a human kidney cell line (S4).

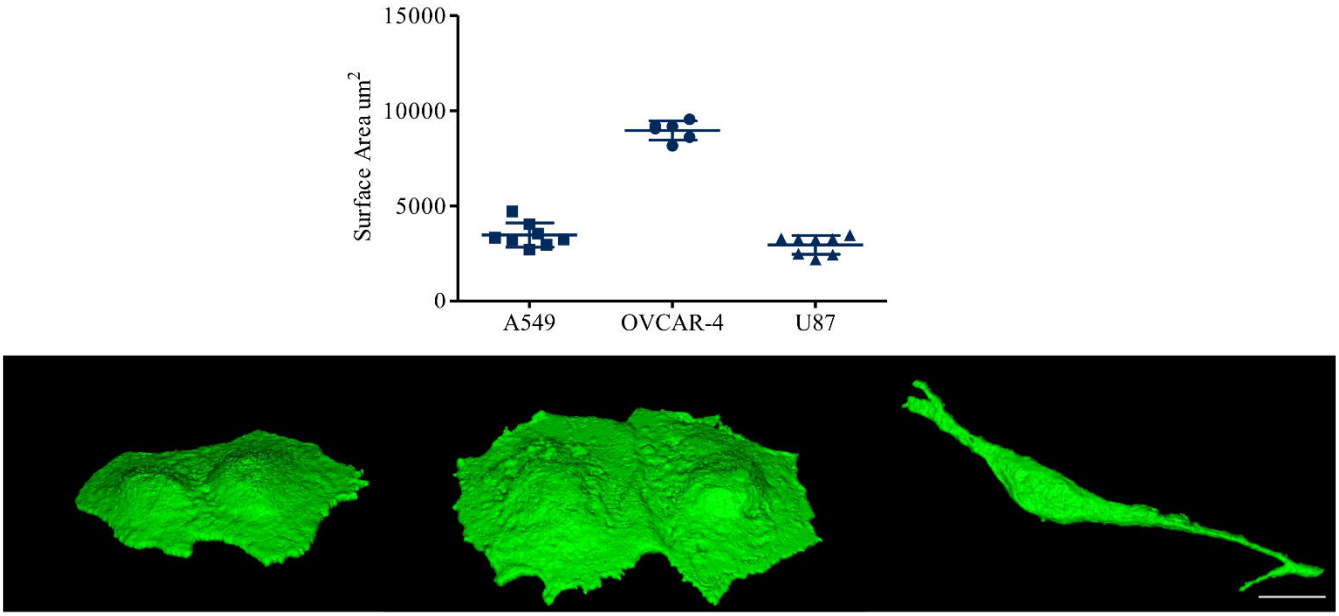

Figure S5: (top) Plot of cell surface area measurements and standard deviation (bottom) 3-D reconstruction of confocal laser scanning microscopy slices of: (left) two A549 cells, (middle) two OVCAR-4 cells, (right) single U-87 MG cell. Scale bar is 20 µm.

Section 3: Internalization of Fluorescent Probe into OVCAR-4 Cells.

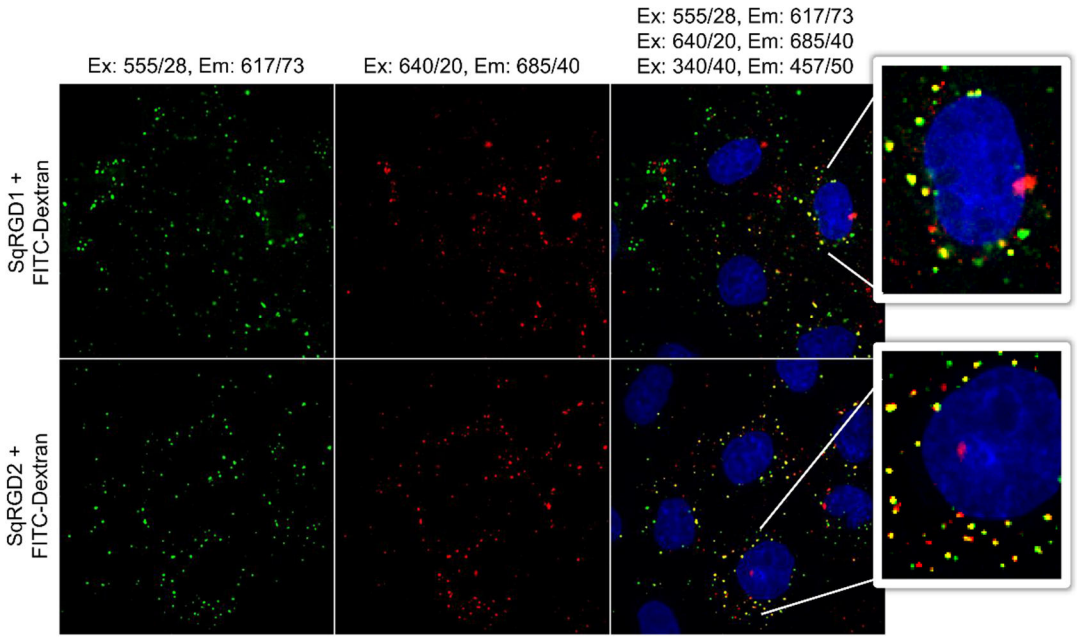

Figure S6: Fluorescent micrographs showing colocalization of SqRGD1 or SqRGD2 with TRITC-Dextran (70 kDa) a known marker for endosomes and lysosomes.

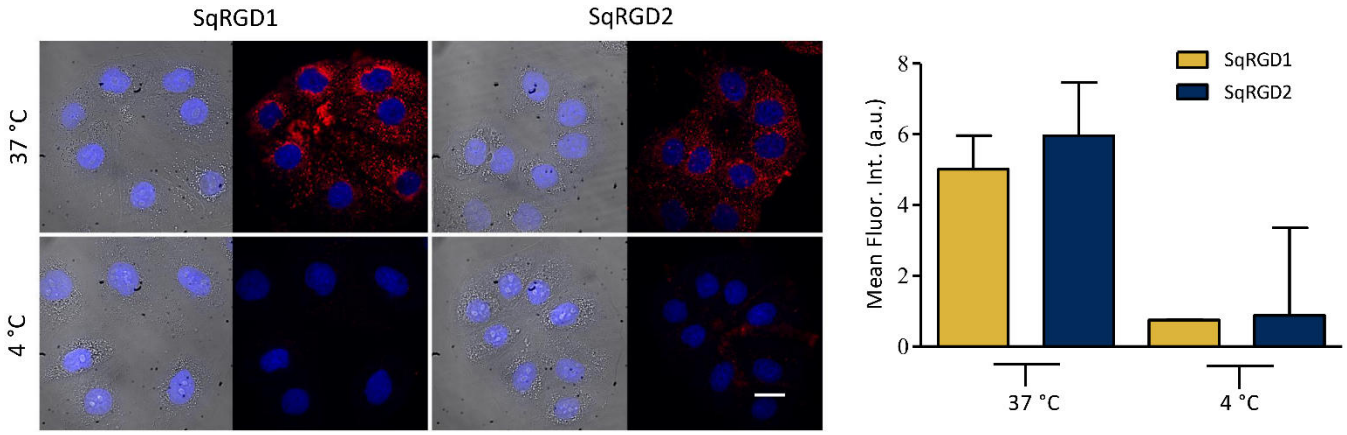

Figure S7: Cell internalization of targeted probes (100 nM) was greatly reduced when the temperature was reduced to 4 °C.

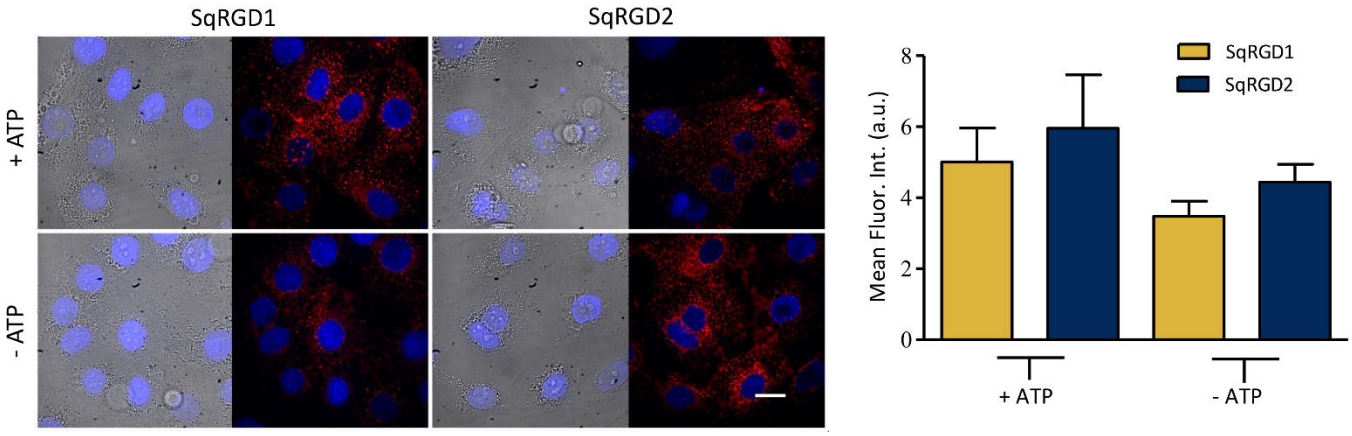

Figure S8: Cell internalization of targeted probes (100 nM) was reduced when intracellular ATP was chemically depleted by presence of sodium azide (0.1%) and deoxyglucose (50 mM).

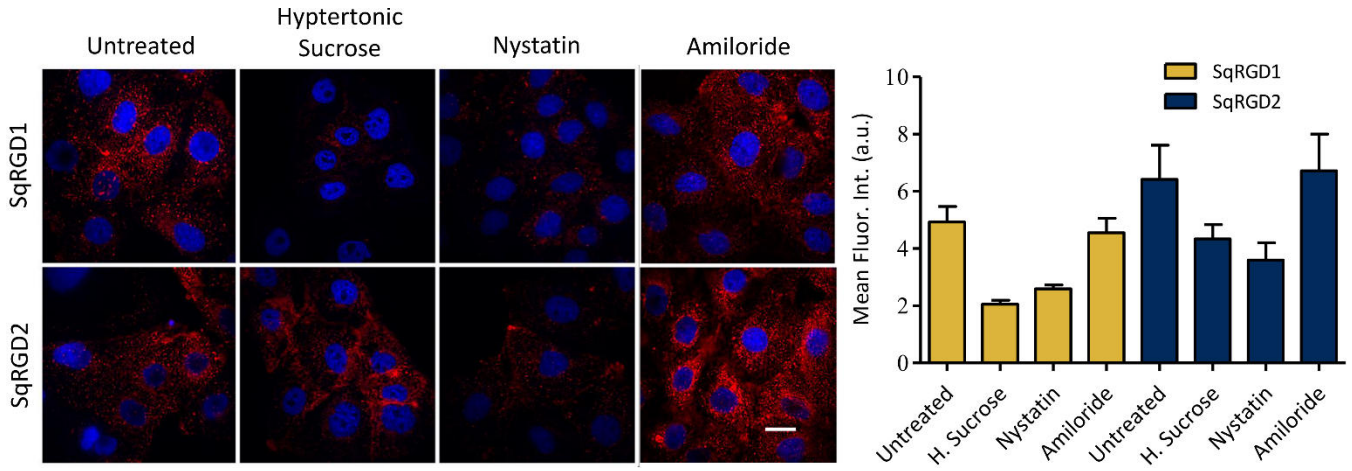

Figure S9: Effect of various chemical inhibitors of different endocytosis pathways. In each case, cells were treated with targeted fluorescent probe (100 nM). Hypertonic sucrose inhibits clathrin mediated endocytosis. Nystatin inhibits caveolae mediated endocytosis. Amiloride inhibits pinocytosis.

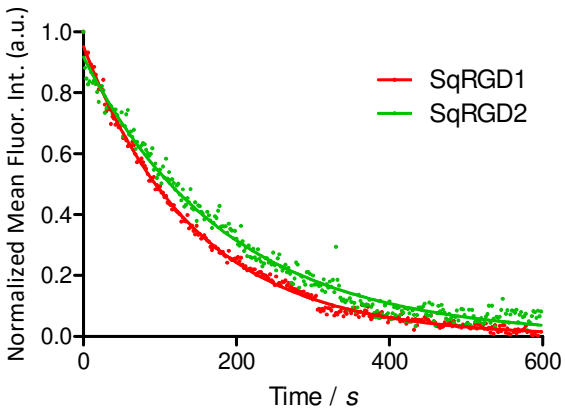

Figure S10: Relative photobleaching of SqRGD1 and SqRGD2 fluorescence from samples of fixed cells undergoing continuous illumination and image acquisition using a Ex: 640/20, Em: 685/40 filter set

Section 4: References

S1. Cahall CF, Lilly JL, Hirschowitz EA, Berron BJ. A Quantitative Perspective on Surface Marker Selection for the Isolation of Functional Tumor Cells. *Breast Cancer (Auckl)*. 2015;9(1):1-11.

S2. Needham D, Hocmuth RM. A sensitive measure of surface stress in the resting neutrophil. *Biophys J*. 1992;61(6):1664-70.

S3. Kubínová L, Janácek J, Karen P, Radochová B, Difato F, Krekule I. Confocal stereology and image analysis: methods for estimating geometrical characteristics of cells and tissues from three-dimensional confocal images. *Physiol Res*. 2004;53(1):47-55.

S4. Sommerhage F, Helpenstein R, Rauf A, Wrobel G, Offenhäusser A, Ingebrandt S. Membrane allocation profiling: a method to characterize three-dimensional cell shape and attachment based on surface reconstruction. *Biomaterials*. 2008;29(29):3927-35.